The Conformation of a Rubbed Polyimide

Roland Meister*

FOM−Institute for Atomic and Molecular Physics, Kruislaan 407, NL-1098 SJ Amsterdam, The Netherlands

Blandine Jérôme

Instituut voor Technische Scheikunde, Universiteit van Amsterdam, Nieuwe Achtergracht 166, 1018 WV Amsterdam, The Netherlands

Received April 15, 1998; Revised Manuscript Received July 21, 1998

ABSTRACT: We report second harmonic generation (SHG) measurements of rubbed and unrubbed surfaces of the fluorinated main-chain polyimide PMDA/BDAF made from pyromellitic dianhydride (PMDA) and 2,2-bis[4-(4-aminophenoxy)phenyl]hexafluoropropane (BDAF). Such rubbed polymers are commonly used as alignment materials for the nematic phases of liquid crystal display cells (LCD), although the rubbing process itself is not yet well understood. The SHG results are used to construct the full orientational distribution function of the noncentrosymmetric part of the polymer. This allows us to determine the preferred conformations of the polyimide at the surface and gives insight into the conformational changes of the polymer during rubbing.

Introduction

Nematic phases are liquids composed of anisotropic molecules, whose long axes are, on average, oriented along the same direction, called the director. Their most important technical application is in displays. These are made of a liquid crystal sandwiched between two glass plates with transparent electrodes, so that the director can be switched by an electric field between two different states. When a voltage is applied, the director orients parallel to the electric field, due to the positive dielectric anisotropy of the nematic phase. In the field-off state, the director switches back to its initial state. This initial state is determined by the preferred orientation of the director imposed by the limiting walls at the interface. The orientations that satisfy a local minimum of the anisotropic interfacial energy act as alignment directions, called anchoring directions.[1]

Rubbed polyimide films are widely used as alignment materials in liquid crystal displays. Many polyimides show a degenerate planar anchoring of nematic phases when the polymer is unrubbed; i.e., the director lies in the substrate plane with no preferred azimuthal direction. To induce a preferred azimuthal orientation, these polyimide layers are rubbed in a given direction with a cloth. The efficiency of this rubbing is characterized by the so-called rubbing strength. After rubbing, the director orients parallel to the rubbing direction. In addition, rubbing also creates a slanted arrangement of the director, which is described by the pretilt angle θ_p, i.e., the angle between the director and its projection onto the substrate plane. For many polyimides the pretilt angle lies in the range of a few degrees and increases with the rubbing strength.[2] However, there are also polymers that show the reverse effect. Here the anchoring of the unrubbed polymer is homeotropic ($\theta_p = 90°$), and the pretilt angle decreases with increasing rubbing strength.[3] Polyimides which induce a high pretilt angle are needed for specially tailored display applications. These materials often contain some fluorinated groups that tend to stick out of the surface of the polyimide.

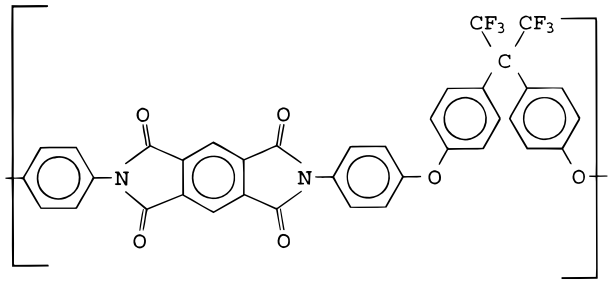

Figure 1. Chemical structure of the polymer PMDA/BDAF. The square brackets enclose the repeat unit.

The effect of rubbing on the polyimide is not yet fully clear. It is believed that an alignment of the polymer chain parallel to the rubbing direction takes place.[4−6] In this respect, rubbing would be similar to stretching of a polymer film, which also leads to an alignment of the polymer chains. This can be concluded from the observed birefringence of polymer surfaces[4,6] after rubbing. Actually, only a surface layer is oriented while the bulk of the polymer (for thick polymer films) still shows an isotropic orientation of the polymer chain.[4,6,7] Contrary to stretching, rubbing also induces a polarity in the surface layer, as rubbing is unidirectional. The resulting polar order of the polymer surface layer has indeed been observed by second harmonic generation experiments (SHG).[8,9]

Depending on the type of polyimide used, different alignment effects due to rubbing can occur for fluorinated polymers. If a polymer has a fluorinated group located in a side chain of the polymer, both the polymer and the side chain can be nicely oriented along the rubbing direction, due to the decoupling effect of the side chain spacer.[8] If, however, the fluorinated groups are located close to or in the main chain, the rubbing produces a competition between the alignment of the polymer chains and the preferred orientation of the fluorinated groups.

We have investigated the effect of rubbing on the surface structure of such a fluorinated main-chain

10.1021/ma980592u CCC: $18.00
Published on Web 12/29/1998

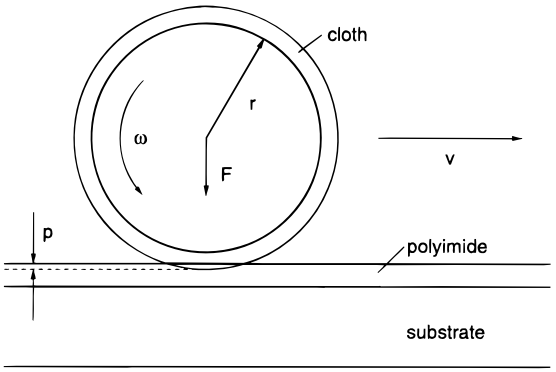

Figure 2. Schematic drawing of the rubbing machine used.

polyimide (PMDA/BDAF) exhibiting a decreasing pretilt angle with increasing rubbing strength. Since the fluorinated groups located at the surface show a polar ordering, we could probe their orientational order using SHG experiments. These measurements allow us to find the preferred conformations of the polymer and give us information about the microscopic orientation mechanism of rubbing.

Experiment and Results

The chemical structure of the polymer is shown in Figure 1. It has been prepared from pyromellitic dianhydride (PMDA) and 2,2-bis[4-(4-aminophenoxy)phenyl]hexafluoropropane (BDAF). The preparation, coating, and rubbing (layer thickness $d \sim 30$ nm) were performed at Philips Research Laboratories (Eindhoven, The Netherlands). In general, rubbing is performed by translating a rotating cylinder (radius r and rotation frequency ω) covered with the rubbing cloth with a constant velocity v over the polyimide surface,[10] sketched in Figure 2. During the rubbing process the cloth is pressed against the polyimide. This leads to an impression of the fibers of the cloth when they are in contact with the polyimide, measured as the pile impression p. For a given type of cloth this is correlated to the force applied to the polyimide surface and therefore characterizes the strength of rubbing. More information about the effect of the rubbing parameters can be found in the literature.[5,10,11] The pile impression for these experiments was varied between $0 \leq p \leq 0.4$ mm while keeping all other parameters of the rubbing process constant.

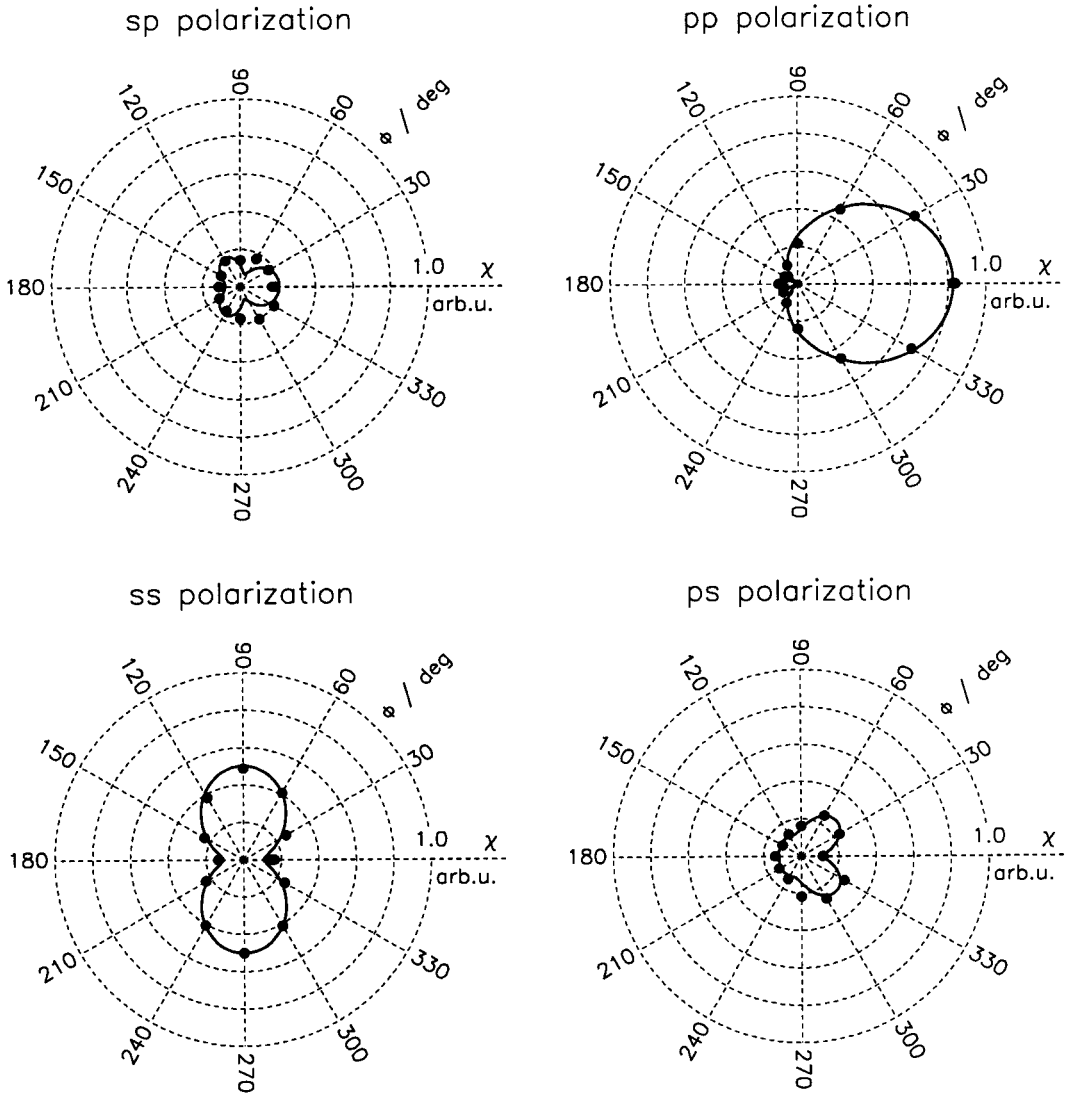

Figure 3. SHG signals as function of the rotation angle of the sample with pile impression $p = 0.3$ mm for sp,pp,ss, and ps polarizations. The first letter refers to the ingoing beam at 532 nm and the second to the outgoing beam of the SHG signal.

The SHG experiments were done with a Q-switched mode-locked Nd:YAG laser. The incident beam had a wavelength of 532 nm, giving a SHG signal at 266 nm. The SHG was measured as function of the rotation of the sample around the substrate normal with rotation angle ϕ. The angle $\phi = 0$ corresponds to the rubbing direction of the polyimide parallel to the outgoing beam. The scans were made for the four combinations of the polarizer settings for incoming and outgoing beam, both polarizations being either parallel (p) or perpendicular (s) to the plane of incidence of the laser beam. Figure 3 shows the experimental results for one rubbing strength, $p = 0.3$ mm.

The theory for SHG generation by surfaces has already been published elsewhere in detail.[12] The SHG signal depends on the second-order nonlinear susceptibility tensor $\boldsymbol{\chi}$, which can be calculated from the second-order nonlinear polarizability tensor $\boldsymbol{\alpha}$. The number of independent components of both tensors depends on the symmetry of the sample and the symmetry of the molecules, respectively.

The symmetry of the unrubbed polymer is $C_{\infty v}$, and in the general case there are four different components in the second-order nonlinear susceptibility tensor $\boldsymbol{\chi}$. The rubbed polymer shows a C_{1v} symmetry; in this case 14 independent components exist. Let us look at the molecular structure of the polymer and identify those parts that allow for SHG generation. We therefore divide the polymer into two different rigid building blocks. The first part consists of the 2,2-biphenylhexafluoropropane subunit and has a triangular shape (**T**). The second part is made of the PMDA units together with the two 4-aminophenoxy groups of the BDAF parts and is a linear unit (**L**). This linear part **L** of the polymer is centrosymmetric and cannot generate a SHG signal. The part **T** shows a C_{2v} symmetry, and the second-order nonlinear polarizability tensor $\boldsymbol{\alpha}$ of this unit has seven independent, nonvanishing components.

Using the full set of components, the interpretation of the results becomes impossible. Therefore, a reduction of the number of elements of $\boldsymbol{\alpha}$ is necessary to decrease the complexity of the system. Let us assume, in analogy to the case of nematogenic molecules at a surface,[12] that the predominant contribution to $\boldsymbol{\alpha}$ comes from the substituted phenyl units of **T** with second-order nonlinear polarizability tensor $\boldsymbol{\beta}$, whose dominating component is $\beta_{\tilde{Z}\tilde{Z}\tilde{Z}}$. The axis $\tilde{Z}$ is oriented along the axis of the phenyl subunit of the triangular unit **T**, as indicated in Figure 4. In a coordinate system XYZ, where the Z axis coincides with the symmetry axis of **T**, the four nonzero components of α are given by (see Figure 4)

$$\alpha_{ZXX} = \alpha_{XZX} = \alpha_{XXZ} = \sin^2(\gamma/2)\cos(\gamma/2)\,\beta_{\tilde{Z}\tilde{Z}\tilde{Z}} \quad (1)$$

$$\alpha_{ZYY} = \alpha_{YZY} = \alpha_{YYZ} = 0 \quad (2)$$

$$\alpha_{ZZZ} = \cos^3(\gamma/2)\,\beta_{\tilde{Z}\tilde{Z}\tilde{Z}} \quad (3)$$

where $\gamma \approx 109°$ is the angle between the two phenyl subunits of **T**.

In the coordinate system xyz of the substrate with z as normal and x as rubbing direction (Figure 5), the second-order nonlinear susceptibility is then given by

$$\chi_{ijj} = N_s\{\langle(\hat{\imath}\cdot\hat{Z})(\hat{\jmath}\cdot\hat{Z})(\hat{\jmath}\cdot\hat{Z})\rangle\alpha_{ZZZ} + [2\langle(\hat{\imath}\cdot\hat{Z})(\hat{\jmath}\cdot\hat{X})(\hat{\jmath}\cdot\hat{X})\rangle + \langle(\hat{\jmath}\cdot\hat{Z})(\hat{\imath}\cdot\hat{X})(\hat{\jmath}\cdot\hat{X})\rangle]\alpha_{ZXX}\} \quad (4)$$

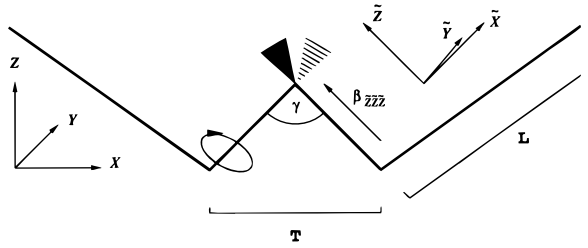

Figure 4. Sketch of the molecular polymer chain structure.

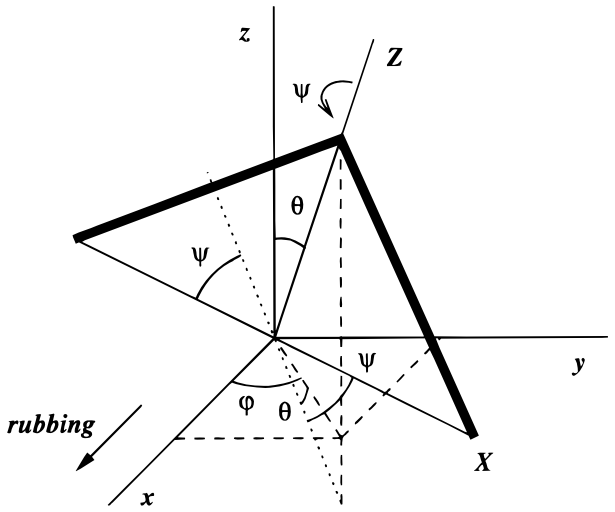

Figure 5. Relation between the molecular (XYZ) and the substrate (xyz) coordinate systems. The angles θ and φ are the polar and the azimuthal angle for the axis Z, while the angle ψ describes a rotation of the coordinate system XYZ around the Z axis. x is the rubbing direction.

Due to the permutation symmetry of eq 4, the number of independent, nonvanishing components of $\boldsymbol{\chi}$ reduces to two for symmetry $C_{\infty v}$ (only χ_{zzz} and $\chi_{zyy} = \chi_{zxx}$ are nonzero) and to six for symmetry C_{1v}. The explicit formulas are

$$\chi_{xxx} = N_s\{\langle(\sin\theta\cos\varphi)^3\rangle\alpha_{ZZZ} + 3\langle(\sin\theta\cos\varphi)\times(\cos\theta\cos\varphi\cos\psi - \sin\varphi\sin\psi)^2\rangle\alpha_{ZXX}\} \quad (5)$$

$$\chi_{xyy} = N_s\{\langle(\sin\theta\cos\varphi)(\sin\theta\sin\varphi)^2\rangle\alpha_{ZZZ} + [2\langle(\sin\theta\sin\varphi)(\cos\theta\cos\varphi\cos\psi - \sin\varphi\sin\psi)\times(\cos\theta\sin\varphi\cos\psi + \cos\varphi\sin\psi)\rangle + \langle(\sin\theta\cos\varphi)\times(\cos\theta\sin\varphi\cos\psi + \cos\varphi\sin\psi)^2\rangle]\alpha_{ZXX}\} \quad (6)$$

$$\chi_{xzz} = N_s\{\langle(\sin\theta\cos\varphi)(\cos\theta)^2\rangle\alpha_{ZZZ} + [2\langle(\cos\theta)\times(\cos\theta\cos\varphi\cos\psi - \sin\varphi\sin\psi)(-\sin\theta\cos\psi)\rangle + \langle(\sin\theta\cos\varphi)(-\sin\theta\cos\psi)^2\rangle]\alpha_{ZXX}\} \quad (7)$$

$$\chi_{zxx} = N_s\{\langle(\cos\theta)(\sin\theta\cos\varphi)^2\rangle\alpha_{ZZZ} + [2\langle(\sin\theta\cos\varphi)\times(-\sin\theta\cos\psi)(\cos\theta\cos\varphi\cos\psi - \sin\varphi\sin\psi)\rangle + \langle(\cos\theta)(\cos\theta\cos\varphi\cos\psi - \sin\varphi\sin\psi)^2\rangle]\alpha_{ZXX}\} \quad (8)$$

$$\chi_{zyy} = N_s\{\langle(\cos\theta)(\sin\theta\sin\varphi)^2\rangle\alpha_{ZZZ} + [2\langle(\sin\theta\sin\varphi)\times(-\sin\theta\cos\psi)(\cos\theta\sin\varphi\cos\psi + \cos\varphi\sin\psi)\rangle + \langle(\cos\theta)(\cos\theta\sin\varphi\cos\psi + \cos\varphi\sin\psi)^2\rangle]\alpha_{ZXX}\} \quad (9)$$

$$\chi_{zzz} = N_s\{\langle(\cos\theta)^3\rangle\alpha_{ZZZ} + 3\langle(\cos\theta)(-\sin\theta\cos\psi)^2\rangle\alpha_{ZXX}\} \quad (10)$$

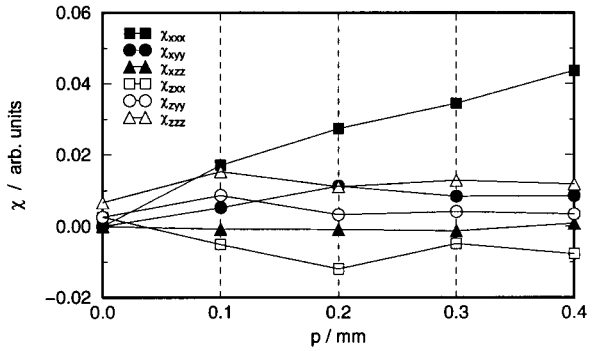

Figure 6. Dependence of the second-order nonlinear susceptibilities χ_{ijj} on the rubbing parameter pile impression p.

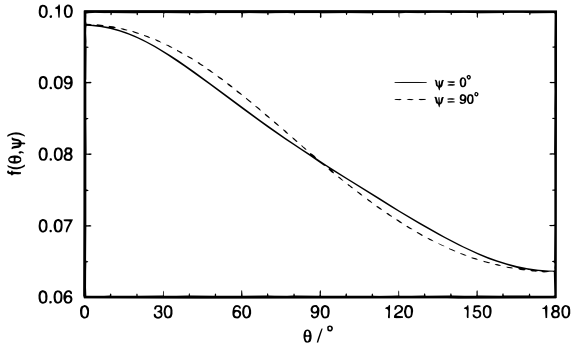

Figure 7. Orientational distribution function $f(\theta,\psi)$ of the unrubbed polyimide.

where (θ,φ,ψ) are the three Euler angles defining the orientation of the reference frame (XYZ) of **T** with respect to the reference frame (xyz) of the substrate. These components of χ can be obtained from the experiments by fitting the SHG scans as a function of the rotation angle ϕ of the sample around its normal with the appropriate formulas. These formulas were already derived in ref 12 for nematic materials and can also be used in the case of this polymer because they relate only to the symmetry of the sample and to the permutation symmetry of the indices. The solid lines in Figure 3 show the curves obtained by a simultaneous fit of all four measurements for one rubbing strength. Figure 6 gives the dependence of the χ_{ijj} as a function of the pile impression p. A clear increase of χ_{xxx} with rubbing strength is observed, while there is hardly any trend for all other parameters, as the experimental and fitting error is in the range 0.005−0.01.

As the six components of the second-order nonlinear susceptibility tensor are related to one predominant component $\beta_{\tilde{z}\tilde{z}\tilde{z}}$ of the second-order nonlinear polarizability tensor, they contain information about some moments of the orientational distribution function $f(\theta,\varphi,\psi)$ of the triangular unit **T**. To generate the most probable distribution from this incomplete set of moments, we used the maximum entropy method.[13] In contrast to earlier studies,[12,13] the experiments contain information not only about the polar angle θ and the azimuthal angle φ defining the orientation of the Z axis but also about the third Euler angle ψ that describes a rotation of the triangle **T** (the XZ plane) around the Z axis (see Figure 5).

During entropy maximization the allowed range for the polar angle θ is often reduced to $0° \le \theta \le 90°$. This restriction is based on the assumption that only dipoles pointing away from the surface contribute to SHG. If a molecule at the surface is oriented such that its dipole points toward the bulk (i.e., $\theta > 90°$), a second dipole of a molecule from the bulk can align antiparallel to it. This pair of molecules is centrosymmetric and therefore does not give a contribution to the SHG. However, there is still a nonzero probability for an unpaired dipole directed toward the bulk, and in our case the full range $0° \le \theta \le 180°$ has to be used to get a distribution function that fulfills the measured six constraints for its moments.

Let us add some notes about the orientational distribution function (ODF). It contains the full information about the orientation of the considered molecule where $f(\theta,\phi,\psi) \sin\theta \, d\psi \, d\phi \, d\theta$ gives the probability to find a molecule in a given orientation range from θ to $\theta + d\theta$, ϕ to $\phi + d\phi$, and ψ to $\psi + d\psi$. All physical quantities that depend on the orientation of molecules can be derived from the ODF by an averaging process, written as $\langle A(\theta,\phi,\psi)\rangle = \int_0^{\pi}\int_0^{2\pi}\int_0^{2\pi} A(\theta,\phi,\psi)\, f(\theta,\phi,\psi) \sin\theta \, d\psi \, d\phi \, d\theta$. Examples of this averaging can be seen in eqs 5−10. This holds for properties that are centrosymmetric, e.g., quadrupolar ordering like the order parameter S of nematic phases,[14,15] but is also true for properties of different symmetry, like a polar orientation at the free surface, which can be probed by SHG. In the following we shall use different plots of the ODF to illustrate the orientation of different parts of the polyimide.

For the unrubbed polyimide, the orientational distribution is constant with respect to φ due to symmetry. Therefore the distribution can be written as

$$f(\theta,\psi) = 2\pi f(\theta,\varphi,\psi) \tag{11}$$

which is shown in Figure 7 for $\psi = 0°$ and $\psi = 90°$. The distribution function for the unrubbed polymer shows its maximum at the north pole; i.e., the Z axis of the subunit **T** is preferrently oriented out of the surface. The dependence on ψ is negligible.

The distribution function for the rubbed polymer depends on all three angles θ,φ,ψ and is difficult to represent graphically. Figure 8a,b shows the reduced distribution

$$f(\theta,\varphi) = \int_0^{2\pi} f(\theta,\varphi,\psi)\, d\psi \tag{12}$$

where an integration over ψ has been performed. This gives the orientational distribution function for the Z axis.

Here the maximum value of f is located at $\mathbf{A} = (\theta \sim 50°, \varphi = 0°)$. This means that rubbing forces the symmetry axis of the triangle **T** toward the surface plane, in the direction of the rubbing. Note, however, that the distribution function is relatively high on a closed loop that follows the path of least descent and goes from the maximum toward the point $\mathbf{B} = (\theta \sim 150°, \varphi = 0°)$ and back, indicated in Figure 8b. To show the dependence on the third angle ψ, Figure 9 presents the distribution function $f(\theta,\varphi,\psi)$ for the two points **A** and **B** and for the saddle point $\mathbf{C} = (\theta \sim 117°, \varphi \sim 45°)$ between these two, also on the path of least descent.

For the two maxima **A** and **B**, the X axis of the group **T** is preferably oriented in the (xz) plane containing the rubbing direction x and tilted with respect to the surface plane by 50° and 150°, respectively. For the saddle point **C**, the X axis is preferably in the plane of the substrate and makes an angle of 45° with respect to the rubbing direction.

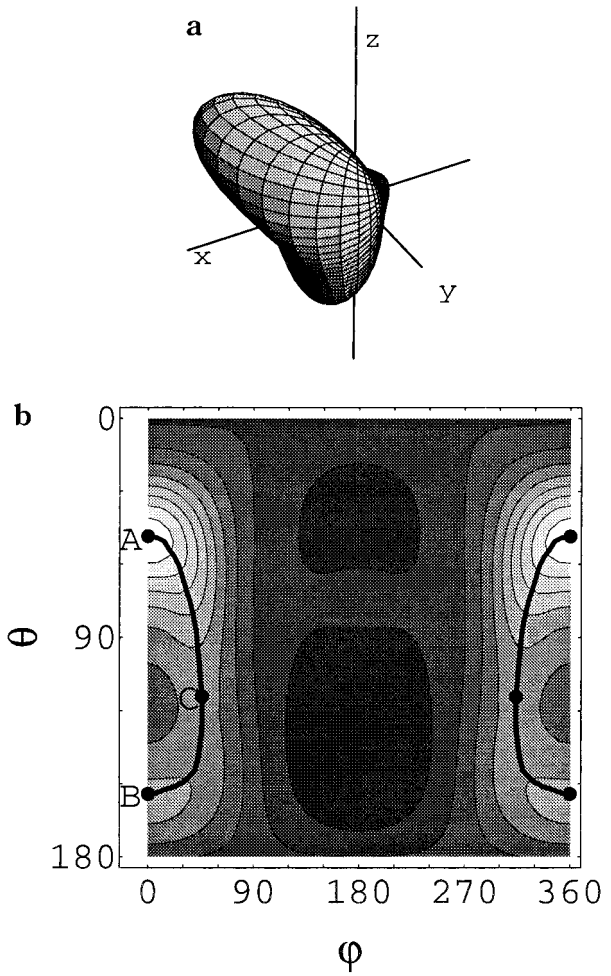

Figure 8. (a) Spherical plot of the reduced orientational distribution function $f(\theta,\varphi)$ for the rubbed polyimide, pile impression $p = 0.4$ mm. The plots for the other rubbing conditions $p = 0.1$, 0.2, and 0.3 mm look very similar. (b) A contour plot of $f(\theta,\varphi)$. The line shows the path of least descent, and the points give the polar and azimuthal angles for the plots of Figure 9.

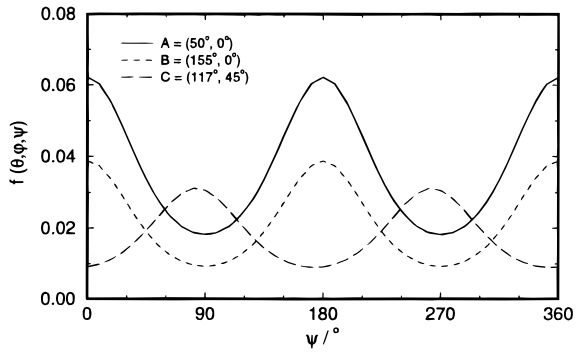

Figure 9. Distribution $f(\theta,\varphi,\psi)$ for different points (θ,φ): **A** (50°,0°), **B** (153°,0°), and **C** (117°,45°). These points are marked in Figure 8b.

Figure 10a shows the dependence of the two maxima on the pile impression p. The graph indicates that these maxima appear already for small pile impressions and that their location does not change much with increasing rubbing strength. The dependence of the value f of the distribution function at these maxima on p is given in Figure 10b. This graph shows an increase of f with p.

To calculate the distribution function for the axis $\tilde{Z}$ of **T**, a third coordinate system $\tilde{X}\tilde{Y}\tilde{Z}$ has to be introduced, where the $\tilde{Z}$ axis is parallel to one of the phenyl groups. The Y and $\tilde{Y}$ axes coincide, and $\tilde{X}$ is the third orthogonal unit vector of this coordinate system (see Figure 4). The distribution function for the $\tilde{Z}$ axis can then be calculated by

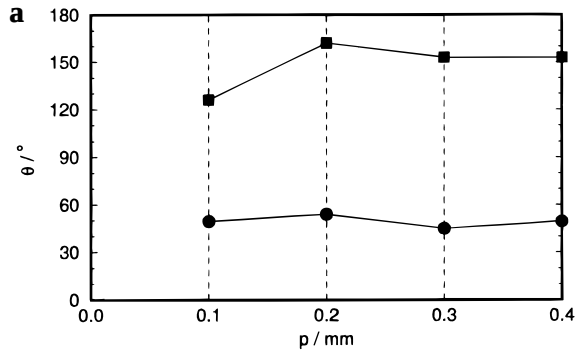

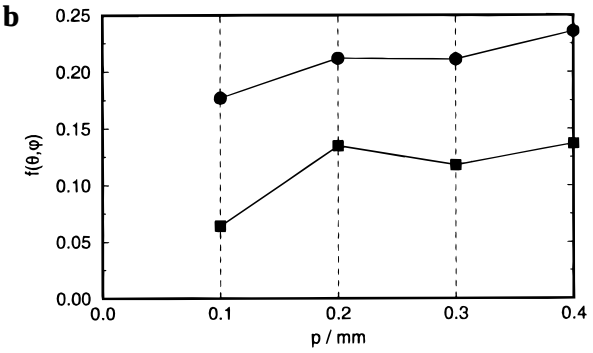

Figure 10. (a) Dependence of the angle θ of (local) maximal distribution density on the pile impression p. The circles refer to point **A** of Figure 8b and the squares to point **B**. (b) Dependence of the value f of (local) maximal distribution density on the pile impression p. The circles refer to point **A** of Figure 8b and the squares to point **B**.

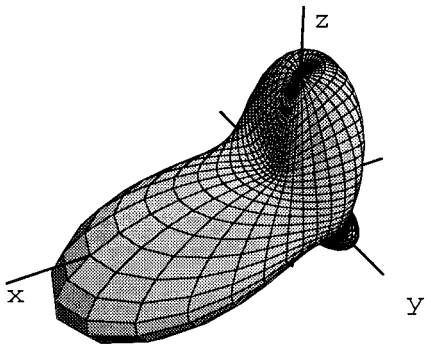

Figure 11. Spherical plot of the reduced orientational distribution function $\tilde{f}(\tilde{\theta},\tilde{\varphi})$ for the rubbed polyimide, pile impression $p = 0.4$ mm.

$$\tilde{f}(\tilde{\theta},\tilde{\varphi}) = \int_0^{2\pi} f(\theta(\tilde{\theta},\tilde{\varphi},\tilde{\psi}),\, \varphi(\tilde{\theta},\tilde{\varphi},\tilde{\psi}),\, \psi(\tilde{\theta},\tilde{\varphi},\tilde{\psi}))\, \mathrm{d}\tilde{\psi} \qquad (13)$$

Mathematically, this is just a change of variables from (θ,φ,ψ) to $(\tilde{\theta},\tilde{\varphi},\tilde{\psi})$ with associated coordinate functions $\theta(\tilde{\theta},\tilde{\varphi},\tilde{\psi})$, $\varphi(\tilde{\theta},\tilde{\varphi},\tilde{\psi})$, and $\psi(\tilde{\theta},\tilde{\varphi},\tilde{\psi})$. The angles $\tilde{\theta}$, $\tilde{\varphi}$, and $\tilde{\psi}$ describe the orientation of the frame $\tilde{X}\tilde{Y}\tilde{Z}$ in the coordinate system xyz, exactly as θ, φ, and ψ describe the orientation of the frame XYZ in xyz. Finally, an integration over the third Euler angle $\tilde{\psi}$ gives the distribution function of the $\tilde{Z}$ axis. Figure 11 shows a spherical plot of $f(\tilde{\theta},\tilde{\phi})$. Figures 12a,b shows the dependence of the maximum of this distribution function on

the pile impression p. Again, the maximum appears already for small rubbing strengths and does not change orientation. Only the magnitude of the distribution function increases with stronger rubbing.

Discussion

Rubbed polymer films of PMDA/BDAF have been studied earlier by X-ray photoelectron spectroscopy (XPS).[3] This method gives the relative occurrence of different atom sorts at the surface. The experiments of ref 3 concentrated on the ratios F/C and N/C, as a function of pile impression. The ratio F/C for thick polyimide films ($d = 30$ nm) decreased with increasing rubbing, very strongly for $0.0 \leq p \leq 0.1$ mm and then only very slowly for $p > 0.1$ mm. This means that the CF_3 groups stick out of the surface before it is rubbed. In the rubbed polyimide, other parts of the polyimide also appear at the surface, and some of the CF_3 groups are forced into the bulk.

In addition, the SHG experiments also yield insight into the effects of rubbing on the polymer chains. Figure 10a,b shows that the reorientation of the polymer chains, represented by the general shape of the distribution function, happens already for quite small pile impressions. The effect of stronger rubbing is a growing asymmetry of the distribution; i.e., a larger percentage of molecules is oriented in the preferred conformations.

A comparison of the results for the ratio N/C is not possible, because the SHG does not give any information about the PMDA part of the polymer where the nitrogen atoms are located.

The polymer PMDA/BDAF cannot be stretched to a straight line because of several kinks in the main chain, which are visible in Figure 4. The only flexible links in the polymer are the ether bonds between the two phenyl groups; see Figures 1 and 4. Therefore, it is a rather rigid system, and the coupling between the orientations of the triangular part **T** and the linear part **L** is rather strong. For the case of rubbed samples this allows one to draw conclusions about the conformations of the main chain from the orientational distribution function of the unit **T** obtained from the SHG experiments by assuming a fairly stretched polymer chain. Figure 13 shows some idealized conformations compatible with the enhanced probability density along the closed curve of Figure 8b. Although none of these sketches exactly match the points **A**, **B**, and **C**, other conformations with a slightly different orientation of the polymer chain also contribute and may in the end lead to the maxima seen in the orientational distribution function. Also, these sketches are idealized with respect to the number of polymer units that construct the repetition sequence. In the sketches this number is two. Surely, more complicated conformation patterns exist, with longer repetition counts. This makes the polymer chain more flexible and allows the **T** units to match the maxima more exactly.

In Figure 13a, the polymer chain lies flat in the substrate area. The other sketches are generated from this conformation by rotating the polymer segments out of this plane but trying to maintain a stretched polymer chain. Figure 13b shows some polymer chain conformations that contribute to point **A**. A polymer conformation that contributes to point **B** is shown in Figure 13c. This last figure clearly reflects the competition between the alignment induced by rubbing and the orientation of the fluorinated groups of BDAF toward the surface, as some of them are forced to be directed into the bulk through stretching.

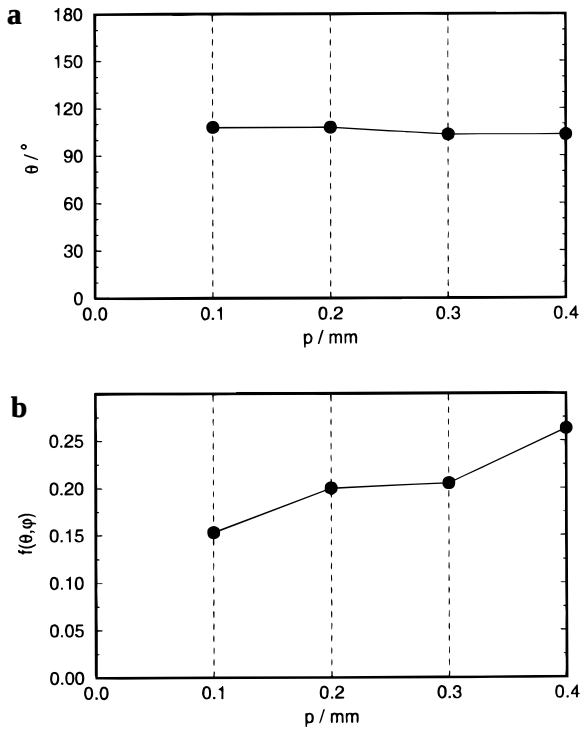

Figure 12. (a) Dependence of the angle $\tilde{\theta}$ of maximal distribution density $\tilde{f}(\tilde{\theta},\tilde{\varphi})$ on the pile impression p. (b) Dependence of the value $\tilde{f}$ of maximal distribution density $\tilde{f}(\tilde{\theta},\tilde{\varphi})$ on the pile impression p.

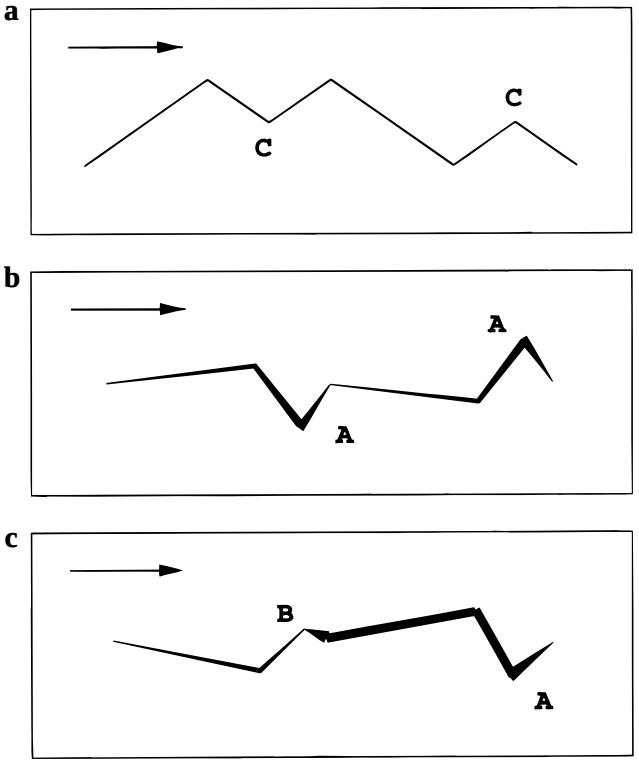

Figure 13. Chain conformations for different orientations of **T**, roughly corresponding to the points **A**, **B**, and **C** of Figure 8b. The sketches give a view onto the substrate area. The thick and thin lines are located before and behind the substrate plane, respectively. The rubbing is indicated by the arrows. For details see text.

A different method to determine the orientations of polymers is by examination of the near-edge X-ray absorption fine structure (NEXAFS). This method is useful to probe the quadrupolar orientation of different

parts of the polyimide, i.e., the centrosymmetric part of the ODF.[16,17] Surface SHG on the other hand is a probe of the polar part of the distribution function. Both methods therefore give complementary information on the orientation of the polyimide at the surface. This difference in symmetry is also reflected in the chemical structure of the polyimides used in our work and those of the literature.[16,17] The polyimides examined with NEXAFS do not show a large polar asymmetry, and we do not expect them to show a SHG signal. For our experiments the triangular part **T** of BDAF/PMDA together with the preference of the fluoro atoms to be located at the air interface creates a polar orientation that is seen by SHG. Nonetheless, the main conclusions from both experiments are quite similar: the polyimide main chain is stretched during rubbing along the rubbing direction, but the orientation axis is not oriented totally within the surface located in the *xy* plane but tilted by a small angle θ_0 out of this plane.[17] A similar result can be seen in Figure 13b,c. But due to the nonlinear shape of BDAF/PMDA, the orientations of **T** and **L** are quite different. Figure 13b,c might even be considered as a "shinglelike" arrangement of the aromatic cores.[17]

The distribution function $f(\tilde{\theta},\tilde{\varphi})$ of the $\tilde{Z}$ axis is also the orientational distribution function of the long axis of the molecules of the nematic phase at the interface, if the alignment mechanism of this polyimide for nematic phases is a parallel alignment of the long axis of the mesogenic molecules and the $\tilde{Z}$ axis of the polyimide. Then $\tilde{f}$ is actually the boundary condition for the anchoring problem of liquid crystals. If it is possible to describe the observed pretilt angles $\theta_p(p)$ as a function of $\tilde{f}(p)$, the supposed anchoring mechanism will be supported. These calculations are currently in progress.

Acknowledgment. This work is part of the research program of the Stichting voor Fundamenteel Onderzoek der Materie (FOM), which is financially supported by the Nederlandse Organisatie voor Wetenschappelijk Onderzoek (NWO). This work has been supported by Stichting voor de Technische Wetenschappen (STW), Grant FAM55.3714. This is a collaboration between Merck (Darmstadt, Germany), Philips Research Laboratories (Eindhoven, The Netherlands), AMOLF, and the University of Amsterdam.

References and Notes

(1) Jérôme, B. *Rep. Prog. Phys.* **1991**, *54*, 391−451.
(2) Uchida, T.; Seki, H. Surface alignment of liquid crystals. In *Liquid Crystals—Applications and Uses*; Bahadur, B., Ed.; World Scientific: Singapore, 1990; Vol. 3.
(3) Cnossen, G.; van der Donk, T. H.; Willard, N. P. *Ferroelectrics* **1996**, *178*, 87−100.
(4) van Aerle, N. A. J. M.; Barmentlo, M.; Hollering, R. W. J. *J. Appl. Phys.* **1993**, *74*, 3111−3120.
(5) Nishikawa, M.; Bessho, N.; Natsui, T.; Ohta, Y.; Yoshida, N.; Seo, D.-S.; Ilmura, Y.; Kobayashi, S. *Mol. Cryst. Liq. Cryst.* **1995**, *275*, 15−25.
(6) van Aerle, N. A. J. M.; Tol, A. J. W. *Macromolecules* **1994**, *27*, 6520−6526.
(7) Toney, M. F.; Russell, T. P.; Logan, J. A.; Kikuchi, H.; Sands, J. M.; Kumar, S. K. *Nature* **1995**, *374*, 709−711.
(8) Shirota, K.; Ishikawa, K.; Takezoe, H.; Fukuda, A.; Shiibashi, T. *Jpn. J. Appl. Phys. 1* **1995**, *34*, L316−L319.
(9) Shirota, K.; Yaginuma, M.; Sakai, T.; Ishikawa, K.; Takezoe, H. *Appl. Phys. Lett.* **1996**, *69*, 164−166.
(10) van Aerle, N. A. J. M. *J. Soc. Inf. Disp.* **1994**, *2*, 41−46.
(11) Seo, D.-S.; Kobayashi, S.; Nishikawa, M.; Hahn, E.-J.; Yabe, Y. *Mol. Cryst. Liq. Cryst.* **1996**, *275*, 37−47.
(12) Feller, M. B.; Chen, W.; Shen, Y. R. *Phys. Rev. A* **1991**, *43*, 6778−6792.
(13) Jérôme, B.; Shen, Y. R. *Phys. Rev. E* **1993**, *48*, 4556−4574.
(14) de Gennes, P. G. *The Physics of Liquid Crystals*; Clarendon Press: Oxford, 1974.
(15) Vertogen, G.; de Jeu, W. H. *Thermotropic Liquid Crystals, Fundamentals*; Springer-Verlag: Berlin, 1988.
(16) Samant, M. G.; Stöhr, J.; Brown, H. R.; Russell, T. P.; Sands, J. M.; Kumar, S. K. *Macromolecules* **1996**, *29*, 8334−8342.
(17) Weiss, K.; Wöll, C.; Böhm, E.; Fiebranz, B.; Forstmann, G.; Peng, B.; Scheumann, V.; Johannsmann, D. *Macromolecules* **1998**, *31*, 1930−1936.

MA980592U